

Assessment of Nigerian Calcium Bentonite as Cement Replacement for Shallow depth Oil Well Cementing Operation

A. O. Arinkoola, S. O. Alagbe*, K. K. Salam, B. M. Ajagbe, I. O. Akinwale

Department of Chemical Engineering, Ladoke Akintola University of Technology, Ogbomosho, Nigeria



ABSTRACT: This study assessed the rheological and mechanical properties of Nigerian Ewu-Obi Calcium Bentonite (ECaB) as cement partial replacement for shallow depth cementing operations using experimental design and response surface methodology. Rheological properties, Thickening Time (TT), and Compressive Strength (CS) were measured using a 12-speed rotational viscometer, High-Pressure High Temperature (HPHT) Consistometer, and Ultrasonic Cement Analyzer, respectively. The effect of the increase in the concentration of bentonite clay as well as its interaction with other cement additives (accelerator and antifoam) on plastic viscosity (PV), yield point (Yp), fluid loss (FL), TT, and CS were investigated. The result shows that the optimum replaceable percentage of ECaB in class G cement, accelerator, and antifoam is 23.5, 7.5, and 0.95 wt %, respectively. At optimum conditions, the PV (17.5 ± 1.35 cp), FL (20 ml/30 min/100 psi), TT (228 ± 16.4 min), and CS24 (614 ± 0.57 psi) obtained agreed with the API standard and compared favorably with literature.

KEYWORDS: Nigerian bentonite, Light weight cement, Optimization, Compressive strength, Local content, Box-Behnken design

[Received Apr. 6, 2022; Revised Jul. 9, 2022; Accepted Jul. 19, 2022]

Print ISSN: 0189-9546 | Online ISSN: 2437-2110

I. INTRODUCTION

Oil and gas well cementing involves the preparation, pumping, and placing of cement slurry between the casing and wellbore annulus for zonal isolation, fluid migration prevention, and protection of casing against corrosion (Arinkoola *et al.*, 2021). Cementing operations in oil and gas are classified into primary and secondary. The primary cementing involves the placement of cement slurry down the annulus between the formation rock and the casing just immediately after landing of the casing. This is to provide zonal isolation, inhibit fluid movement, and for safeguarding the casing against corrosion (Lavrov, 2017). The secondary cementing includes all the corrective operations such as squeeze cementing and plug-back after primary cementing.

Well cementing can be challenging especially in difficult terrains such as weak formations, and fluid-bearing zones (Adjei and Skalle, 2021). Several measures such as use of highly ductile cement slurry have been highlighted to mitigate or avoid some of these challenges (Alkinani *et al.*, 2018; Xinniu, *et al.*, 2019). The best mitigating approach is by developing a cement slurry having a necessary hydrostatic column higher than the pore pressure but lower than the formation fracture pressure (Wu, *et al.*, 2020). Because of the challenges that can be encountered at shallow depth, the use of standard oil-well cement design has been discouraged for zonal isolation owing to the low formation strength (Anya, 2018). One of these challenges is the lost of cement while in

circulation in the bore hole. Lost circulation phenomenon occurs when there is a partial or extremely severe incidence of slurry loss to the formation (Elmarsafawi *et al.*, 2007; Fidan *et al.*, 2004). The incidence often occurs at shallow depth since the formation pressures at such intervals are lower than the hydrostatic pressure associated with the normal high-density cement systems. According to Cook *et al.*, (2011), the cost associated with the occurrence of this phenomenon ranged between 2 to 4 billion USD each year. When it occurs the mud and cement losses in circulation will increase the drilling cost by increasing non-productive time and at times warrant embarking on expensive remedial and workover jobs (Elmarsafawi *et al.*, 2007; Magzoub *et al.*, 2020). In practice, loss circulation intervals once identified are sealed using cement plugs and non-cement sealants. The use of cement plugs however, require higher pumping pressures which can compound the problem by breaking down weak formations and causes fracturing of the formation (Wang, *et al.*, 2017).

To overcome aforementioned challenges, the use of lightweight pozzolanic materials as a fractional replacement for Portland cement has been documented (Yuhuan *et al.*, 2016). Lightweight materials such as fly ash, silica fume, metakaolin, ground granulated blast furnace slag, expanded perlite, zeolite, vermiculite, etc. have been investigated in this regard (Valcuende *et al.*, 2015; Bouaissi *et al.*, 2020; Adjei *et al.*, 2020; Arinkoola *et al.*, 2021). However, low compressive strength of the resulting cement when compared with the standard cement slurries remains a major drawback associated with partial substitution. Nevertheless, the study by Malyshev

*Corresponding author: soalagbe@lautech.edu.ng

et al., (2013) has shown that compressive strength in the range of 250–1000 psi is sufficient to meet the requirement of many cementing operations. Enhanced compressive strength can be obtained by using extenders. The most common extender that is being used and recommended by American Petroleum Institute (API) is Wyoming bentonite.

Wyoming bentonite has unique characteristics that are rarely found anywhere else, it can swell up to 16 times its original size and absorb up to 10 times its weight in water (James *et al.*, 2008) However, the continuous importation from overseas of bentonite for drilling and cementing operations is not only unsustainable but also portends danger for the future socio-economic wellbeing of Nigeria. Bentonite clays from different parts of the world are currently being evaluated as extenders in drilling and cementing. Adjei *et al.*, (2021) evaluated calcined Saudi calcium bentonite as cement replacement in a low-density oil-well cement system and concluded that calcined calcium bentonite exhibit a similar effect as that prepared with fly ash in terms of rheology, thickening time, and compressive strength. Salam *et al.* (2022) examined bentonite clays from Ibeshe, Lukosi and Ewu-Obi deposits located in the South-Western part of Nigeria for cementing operations. The results from their study show all clay samples from these deposits were unsuitable in their raw form in terms of exchangeable cations. Only the bentonites from Ibeshe responded after the beneficiation. Calcium based cement can achieve energy savings as high as 25% and provide environmental benefits by reducing CO₂ emissions by around 20% (Imbabi *et al.*, 2012).

Beneficiation of calcium or potassium-based bentonites to the standard required can be very expensive and hence, increase the cost of drilling. However, utilization of raw bentonites for cementing operations will not only reduce the cost but also hasten the acceptability and encourage adoption of local clays as sustainable alternatives to imported Wyoming bentonites. Therefore, this study assessed the rheological and mechanical properties of Nigerian Ewu-Obi Calcium Bentonite (ECaB) as fractional cement replacement for shallow depth cementing operations using experimental design and response surface methodology. This study is justified because of the abundance of bentonite deposits in Nigeria and the fact that majority of these deposits are calcium based requiring further treatments before use for drilling and other operations.

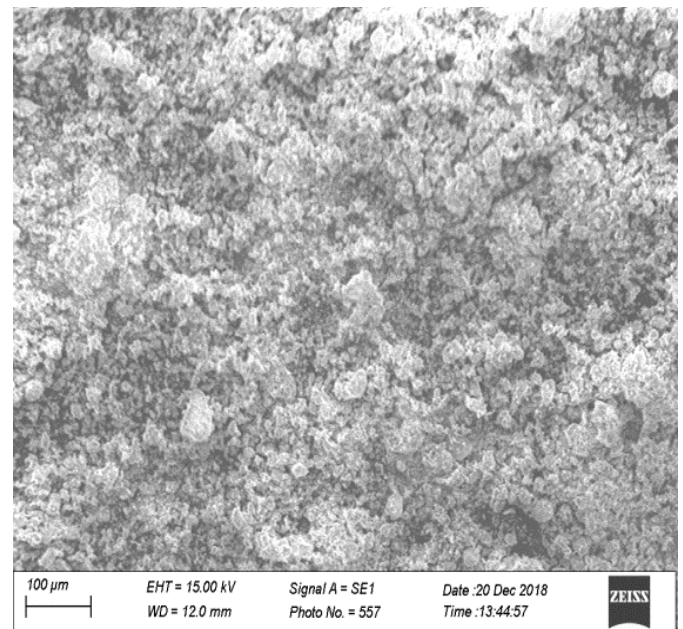
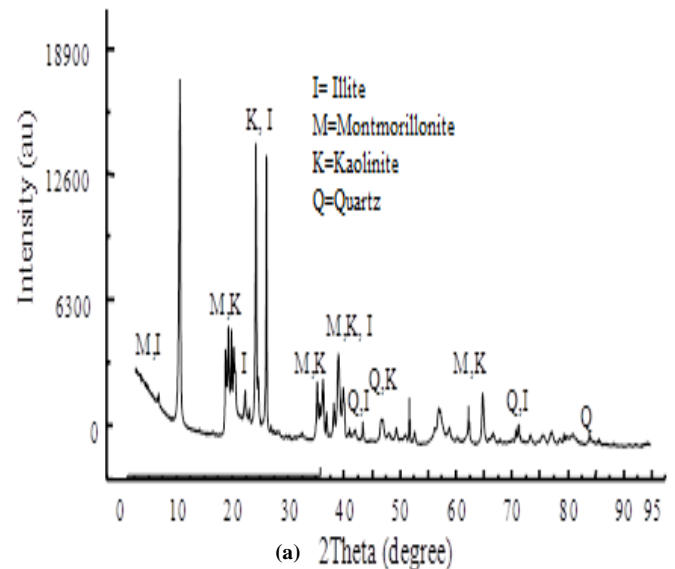
II. METHODOLOGY AND METHODS

A. Materials

The cement additives and the Class G oil well cement was provided by SOWSCO oil well service (Nig.) Ltd, Port Harcourt, Nigeria. Class G cement was selected due to field acceptability and compatibility with the additives. The calcium bentonite was sourced from Ewu-Ebi (6° 32' 51.54" N, 3° 30' 54.828" E) in Lagos State, Nigeria through the Nigerian geological survey. The particle size distribution of the cement shows that approximately 87% have sizes less than 60 µm. Also, about 90% of the raw clay sample has a particle size of

less than 67.9 µm. The XRD analysis revealed that montmorillonite, kaolinite, Illite, and quartz are the dominant minerals in the bentonite with prominent peaks observed at 2θ values of 8.90, 19.58, 34.92, and 62.25° (Figure 1a) at corresponding d-spacing of 4.50, 3.59, 2.46 and 1.49 Å°, respectively. The SEM micrograph of the raw bentonite sample shows closely packed clay aggregates with irregular-shaped surfaces (1b).

The breakdown of chemical composition of the raw ECaB, class G cement, and the imported bentonite is shown in Table 1.



(b)
Figure 1. (a) XRD and (b) SEM Micrograph of raw Ewu-Ebi clay sample.

It can be seen that the ratio of Na₂O/CaO in the raw ECaB is 0.01. The total amount of SiO₂, Al₂O₃, and Fe₂O₃ in the raw ECaB is 74.07 % which makes these materials pozzolanic (ASTM C618-12a, 2010). Typical of all the pozzolanic, the

total percentage of CaO, SiO₂, and Fe₂O₃ in the class G cement is 84.9%. All pozzolanic materials have SiO₂, Fe₂O₃, and Al₂O₃ as key oxides and may contain minor amounts of K₂O, Na₂O, SO₃, MgO, MnO, or TiO₂ (Adjei, *et al.*, 2021).

viscosity (PV) and yield point (Yp) were calculated using Eqns. (3) and (4).

$$PV (cp) = 1.5 * (\theta_{300} - \theta_{100}) \quad (3)$$

$$Yp (lbs/100ft^2) = PV - \theta_{100} \quad (4)$$

Table 1: XRF analysis of cement and bentonites.

	SiO ₂	Al ₂ O ₃	Fe ₂ O ₃	MnO	MgO	CaO	Na ₂ O	K ₂ O	TiO ₂	P ₂ O ₅	LOI
Class G cement	19.53	3.25	7.29	0	1.05	62.12	0	1.3	0	0	5.46
IB	48.8	15.54	6.44	0.07	3.5	5.22	2.19	0.75	0.49	0.13	15.73
ECaB	40	27.55	3.5	0.1	2.5	3.12	0.15	0.12	0.25	0.13	22.5

B. Experimental Procedure

The cement slurry was prepared according to API standards (API SPEC 10A, 2019). The variables in the mix are the extender (ECaB), accelerator, and the antifoam. The solid additives were expressed as a percentage by weight of cement (BWOC) and the liquid additive in gallons per sack of cement. Seventeen stable cement slurries were produced using the Box-Behnken design of experiment (Design-Expert version 11). The ECaB, accelerator, and antifoam were randomized in the range between (16 – 31wt. %), (5 – 10wt. %), and (0.5 – 1.4wt. %), respectively. The dispersant was fixed at 0.9 wt. % in all the mix. Table 2 shows the design matrix (in coded form). The “-1”, “0”, and “+1” denote the minimum, mid value and maximum level of each of the variables, respectively.

Mass balance calculations was carried out on each of the samples using Eqns. 1 and 2 to establish the validity of each of the experimental runs. The slurry density and yield obtained for all the 17 samples produced ranged between 12.1 - 13.8 ppg, and 1.9 – 3 ft³/sack, respectively. This range of density is desirable for safe operation at shallow depth compared with the density of a typical standard oil-well cement (14.8–15.6 ppg).

$$\text{Slurry Density (ppg)} = \frac{\text{Total Weight (lb)}}{\text{Total Volume (gal)}} \quad (1)$$

$$= \frac{\sum \text{Weight of all the slurry components (pounds)}}{\text{Total Volume}}$$

$$= \frac{\sum \text{Volume of all the slurry components (gallons)}}{\text{Total Volume}}$$

$$\text{Slurry Yield (ft}^3\text{)} = \frac{\text{Total Volume (gal)}}{7.48 \text{ (gal/ft}^3\text{)}} \quad (2)$$

Volume (gal) = Weight of the component in gallon
(lb)*Absolute volume of the component
7.48 (gal/ft³) is the conversion factor.

C. Measurement of Thickening Time and Rheology

The Thickening Time (TT) test was carried out using a High-Pressure High Temperature (HPHT) Consistometer (model 7720) at 3,500 psi, bottom hole static temperature (BHST) of 115 °F, and bottom hole circulating temperature (BHCT) of 100 °F. A 12-speed rotational Viscometer was used to measure the rheology of the cement slurries. The plastic

D. Measurement of Compressive Strength and Fluid Loss

Compressive strength was measured using Ultrasonic Cement Analyzer (UCA, model 4265) after 12 and 24 h of curing. The curing condition was done considering downhole pressure of 3,500 psi, BHST of 115 °F, and BHCT of 100 °F. The fluid lost was determined using high pressure and high-temperature filter press operated at 3500 psi and bottom hole static temperature of 115 °F.

E. Data Analysis

Each of the 17 slurries formed was analyzed for TT, Compressive Strength (CS), PV, Yp, and Fluid loss (Table 2). To do this, the adequate model was selected considering the F and p statistics and pertinent independent variables were identified using analysis of variance (ANOVA) at a 95 % confidence interval (α = 0.05). The F-value explains the level of error/noise in the result while the p-value indicates the level of significance of the model and factors. A high value of F or low p-values indicates a low level of noise in the data and a confirmation of the acceptability of the result. The ANOVA involves hypothesis testing. In this study, several models were investigated including linear, quadratic, cubic, and factorial. The two hypotheses that were tested include:

(i) the null hypothesis: all treatments are of equal effects.

$$H_0: \beta_1 = \beta_2 = \dots \beta_K = 0$$

(ii) the alternative hypothesis: some treatment is of unequal effects.

$$H_1: \beta_j \neq 0 \text{ for at least one } j$$

To reject null hypothesis H₀, at least one of the model/variables must explain significantly the variability observed on the responses.

III. RESULTS AND DISCUSSION

A. Model Development

The result obtained from the analysis of the 17 cement formulations is summarized as presented in Table 3. The quadratic model was suitable as evidence in the values of F, p, and correlation coefficients (R-square and Adjusted R-squared). The F-value represents the ratio of signal to noise and a higher value indicates little or no noise which is desirable. The p-values are less than 0.05 in all cases which suggests reliability of at least a 95% confidence limit. The correlation coefficients are all high and close to 1 which indicates the

Table 2: Design matrix for the Box-Behnken design.

Run	X ₁ (%)	X ₂ (%)	X ₃ (%)	TT (min)	CS (psi)	PV (cp)	Yp (lbs/100ft ²)	Fluid Loss (ml/30 mins)
1	1	-1	0	330	651	18.5	29	25
2	-1	0	-1	225	702	15	37	20
3	0	0	0	245	600	16	23	16
4	-1	-1	0	345	662	20.5	33	22
5	1	0	1	270	501	22.5	27.7	20
6	0	0	0	300	579	17	20.5	28
7	0	0	0	300	603	23	29.5	22
8	0	-1	1	340	721	23.5	22	20
9	0	1	1	270	702	13.5	25.5	25
10	-1	0	1	305	681	22.5	22.5	28
11	-1	1	0	285	700	21.5	32	25
12	0	-1	-1	345	751	16.0	24.5	27
13	0	0	0	330	771	19.5	22.5	20
14	0	0	0	330	770	19.0	22.5	20
15	1	1	0	275	561	16.5	29.5	25
16	1	0	-1	325	602	16.5	21.5	25
17	0	1	-1	290	652	23.5	26.5	20

Table 3: Analysis of variance.

	MODEL	SSE	MSE	F-value	p-value	R ²	Ad R ²
TT	QUADRATIC	24618.99	2735.44	22.21	0.0002	0.9662	0.9227
CS	QUADRATIC	45386.44	5042.94	29.18	< 0.0001	0.974	0.9407
PV	QUADRATIC	171.26	19.03	17.07	0.003	0.9685	0.9117
YP	QUADRATIC	250.37	31.3	17.29	0.0013	0.9584	0.903
FL	QUADRATIC	288.86	32.1	27.96	0.0003	0.9767	0.9418

goodness of fit and that the developed models are a good proxy of the experimental data. The generalized coded quadratic correlation is represented by Eqn. (5).

$$y = \gamma_0 + \gamma_1 X_1 + \gamma_2 X_2 + \gamma_3 X_3 + \gamma_4 X_1 X_2 + \gamma_5 X_1 X_3 + \gamma_6 X_2 X_3 + \gamma_7 X_1^2 + \gamma_8 X_2^2 + \gamma_9 X_3^2 \tag{5}$$

where, y represents the various dependent variables (TT, CS, PV, Yp and FL) and γ_i the coefficients of the independent main-effect (X_i), the interaction-effect (X_{ij}) and the quadratic-effect (X_i^2) as shown in Table 4.

the dominant effect on the TT followed by the antifoam (x_3) and then the ECaB (x_1) with -3.13 and 1.88, respectively. Similarly, x_1 shows the largest effect on the CS of the hardened cement followed by x_2 then x_3 . Both the PV and Yp are highly sensitive to x_3 followed by x_1 and then x_2 while the FL are influenced by x_3 , x_2 , and x_1 in that order.

It should be emphasized that the positive or negative signs associated with these coefficients is pointing to the direction of impact on the response. For example, the negative sign that came with the x_2 (-30) in the case of TT indicates that as the wt% of x_2 increases in the mix, the TT decreases. On the other hand, the slurry TT would increase if the wt% of x_1 with +1.88 coefficient is increased.

Table 4: Coefficients of independent variables in Equation 5.

Factor	γ_i				
	TT (min)	CS (psi)	PV (cp)	YP (lb/100 ft2)	FL (ml/30 min/100 psi)
Intercept	239.4	601.8	15.4	22.8	16.4
X1-ECaB	1.88	-31.25	-1	-2.13	0.375
X2-Acc	-30	-21.25	0.75	-0.0625	0.9375
X3-AntF	-3.13	10	1.75	-2.19	1.31
X1X2	1.25	-32.5	-1.38	0.375	-0.75
X1X3	-10	25	1.12	2.63	0
X2X3	-3.75	20	-6.13	4.8	1.37
X12	31.55	0.35	3.11	1.82	6.49
X22	37.8	40.35	-0.3875	6.25	1.36
X32	34.05	62.85	2.11	0	3.61

B. Sensitivity of Main Factors to Cement Properties

The value of estimated coefficients presented in Table 4 indicates the degree to which they influence cement properties. The larger the coefficient value the larger the effect. For example, the accelerator (x_2) with a coefficient, of -30 shows

This explanation goes with the other factors for various responses and this is shown in Figure 2. It can be seen from Figure 2 that the three main factors (x_1 , x_2 and x_3) exhibit no unique pattern of influence on the properties of the cement slurry. The CS is highly sensitive to x_1 than x_2 which exhibits

high influence on TT. The values of PV and FL from the slurry can be influenced by x_3 which show a positive effect. The synergistic effects (x_1x_2 , x_1x_3 and x_2x_3) of these factors can also influence the mechanical and rheological properties as can be seen in Figure 2.

with CS decreasing with an increase in the level of MK dosage (Yuhuan *et al.*, 2016). The effect of the ECaB on the plastic viscosity and FL is illustrated in Fig. 3(c) and Fig. 3(d), respectively.

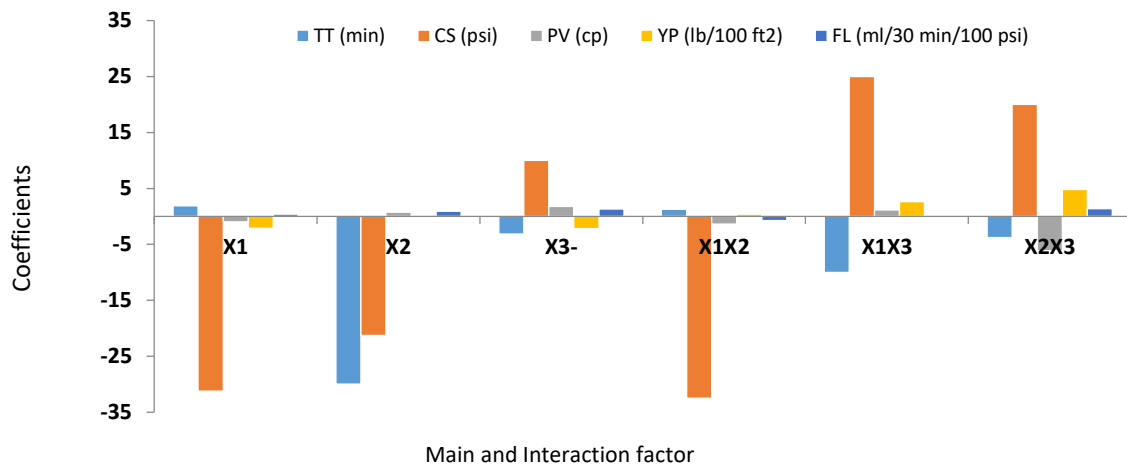


Figure 2: Pareto chart showing the effects of main and interaction factors on the properties of cement slurry and hardened cement.

C. Effect of Calcium Bentonite on Cement Properties

The effects of different dosages of ECaB on TT, CS, PV, and FL of cement slurries are shown in Figure 3. It can be seen from Figure 3 that except for the CS, the cement properties initially degrade with increase in the content of ECaB in the mix until the concentration got to between 22-25% that it started to rise. The TT plot shown in Figure 3 shows a decrease from 270-240 min as ECaB increases from 16-24 g. Thus, the setting time of the slurry reduces with the increasing content of the bentonite clay. This observation was similar to the report by Arinkoola *et al.*, (2021) which indicated a reduction of TT on replacement of Ordinary Portland Cement (OPC) using 15wt% metakaolin. The reduction of TT can be desirable where an early setting is needed such as that at shallow depth. A proper design of cement must consider the appropriate setting time to avoid costly and time-consuming secondary cementing operation. Too long TT could lead to costly delays and increase the operating costs. Too short TT, however, leads to premature setting in the casing or pumping equipment (Coveney, *et al.*, 1996; Arinkoola, *et al.*, 2021). Therefore, the observed sudden increase in TT from 245-280 min by increasing ECaB in the mix from 24-31 g could be traced to the synergistic effects of the additives. Antifoams are used primarily to prevent air entrapment, a study has shown that defoamer reduces the setting time (Morsy, *et al.*, 2012).

The CS of hardened pastes made by partial substitution of Class G cement with different dosages of ECaB after 12 and 24 h is shown in Fig. 1b. The trends of the cement's CS observed after 12 (CS12) and 24 h (CS24) of curing revealed that the CS increased with time. It is higher at 24 h but decreases with increasing dosage of ECaB at the test temperature. A similar observation was made with Metakaolin

It can be seen that the PV reduces with an increase in the amount of ECaB in the mix, up to a level at which a further increase leads to a rise in the PV. The result from this study agreed well Shahriar and Nehdi, (2012). The authors reported a decrease in cement PV with an increase in fly ash. However, Bu *et al.* (2016) has reported that metakaolin, silica fume, and rice husk ash all show increasing PV when used between 10-15% in the cement mix. A reduction in PV is advantageous because much lower energy would be required to pump the cement slurry down the hole. It should be emphasized that ECaB above 25 % induces an increase in PV and FL. Therefore, there is a need for determining optimum ECaB and other additives that would guarantee acceptable PV and FL without compromising the CS and TT of the cement slurry.

D. Synergistic Effects of Factors on CS and TT of Cement

The interaction graph showing the synergistic effects of ECaB, antifoam (x_3), and accelerator (x_2) on CS and TT of slurry and hardened cement is shown in Figure 4. It can be seen that interaction occurs by the changes observed in the various responses as one factor was kept low or high while the other is increasing or decreasing within its limit. It is observed from Figures 4(a) and 4(b) that the effects of x_1 and x_2 on the CS, TT, and PV when interacting with ECaB are relatively significant. The effect of the x_3 on the CS of hardened cement when interacting with the x_1 is substantial as shown in Fig. 4a. When x_3 was added to the mix in high dosage, an increase of x_1 between 16-33 g showed little effect on CS. But low dosages of x_3 in the mix, any increase of x_1 resulted in a dramatic reduction of the CS. Conversely, a relatively low

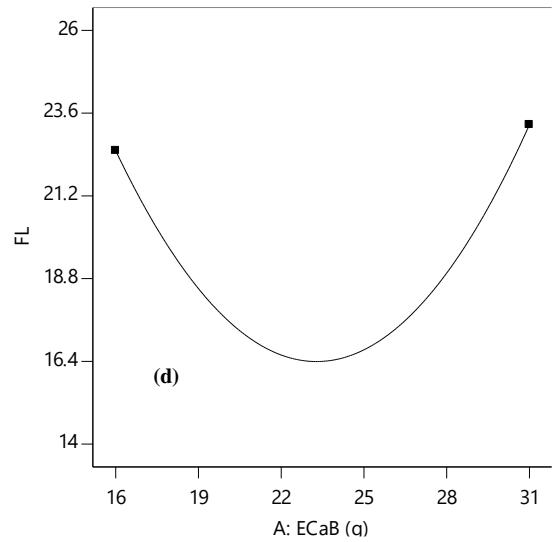
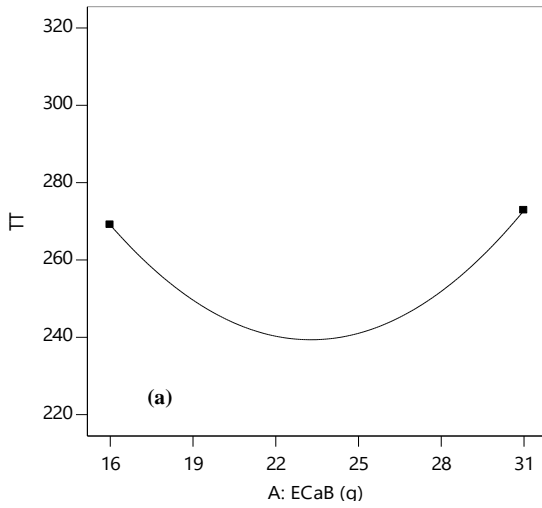
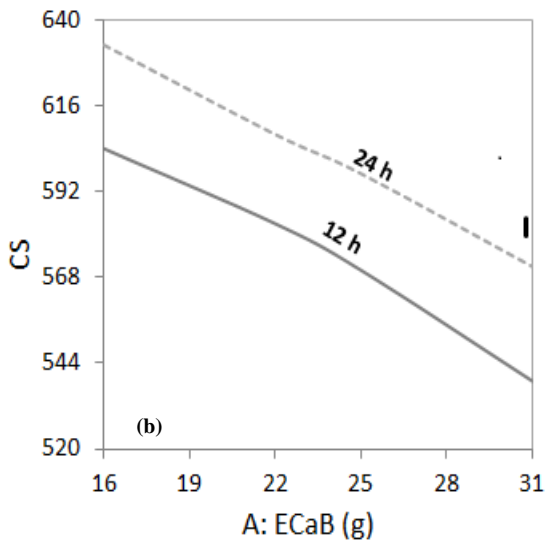
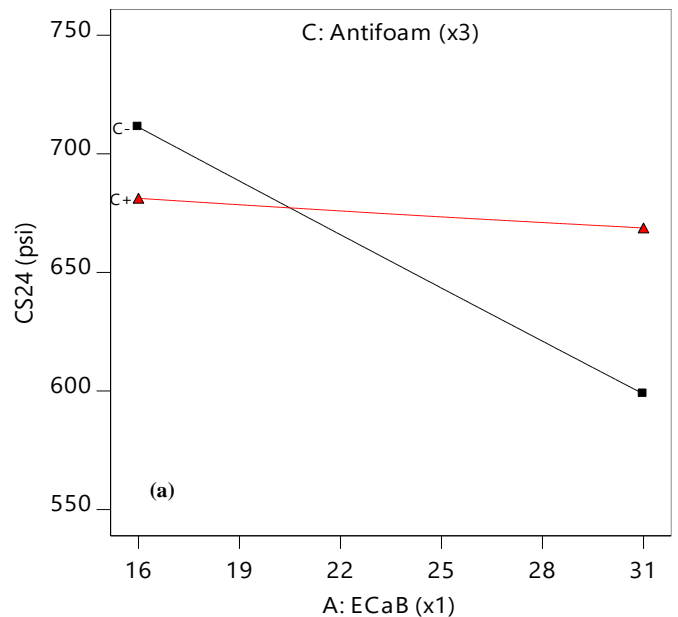
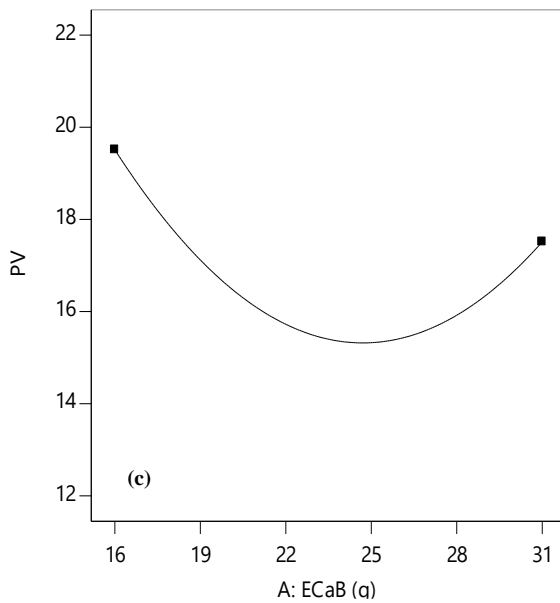


Figure 3: Effects of different dosages of ECaB on (a) TT, (b) CS, (c) PV, (d) FL.



dosage of x_2 ensured more stability of CS as x_1 substituted in the OWC increases between 16-31 g.

The effect of the interaction of x_1 on slurry TT when low and high dosages of x_2 and x_3 were incorporated into the cement slurry is shown in Figures 4(c and d). As observed in Figure 4(c), to achieve a reasonable amount of x_1 in OWC, a relatively low dosage of x_3 is required in the mix. Also, to achieve a reasonable delay of TT for effective cement placement, a relatively low dosage of x_2 is required as evidenced in Figure 4(d).



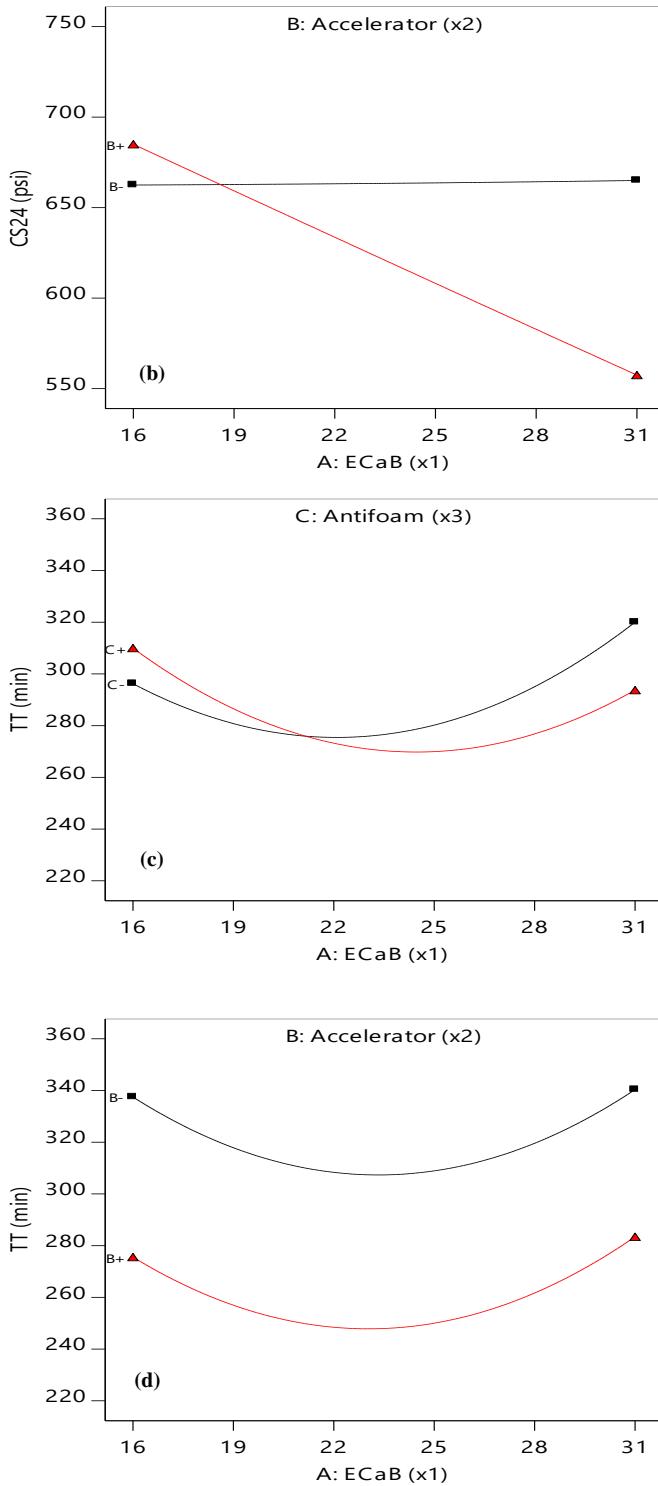
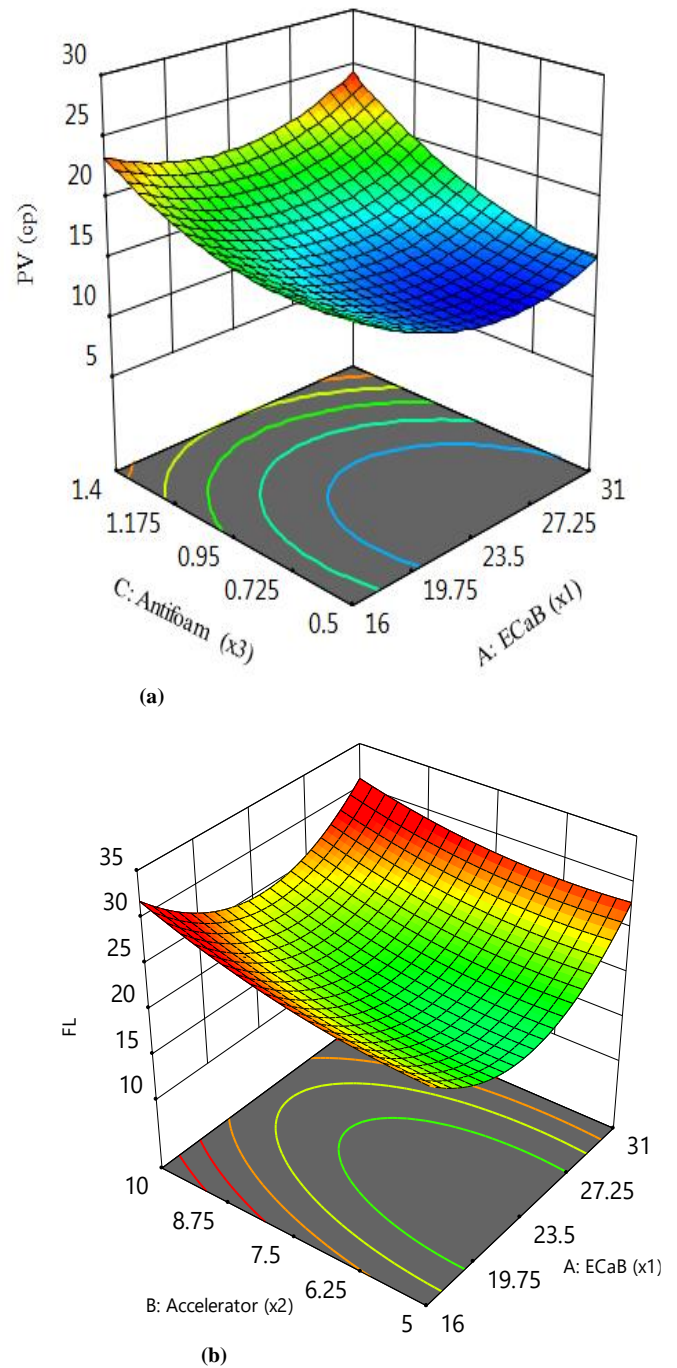


Figure 4: Interaction graph showing the effects of ECaB dosages for different levels of antifoam (x₃) and accelerator (x₂) on CS and TT of slurry and hardened cement.

The 3D surface plots that further explain how x₁ interacted with x₂ and x₃ are shown in Figure 5 (a-c). It is clearly seen from Fig. 5(a) that, the effect of x₁ on the PV of the cement slurry varies depending on the quantity of x₃ in the mix. Thus, there was a synergy between x₁ and x₃ as far as PV is concerned. The PV of the cement is higher with a high

amount of x₃ and lower for a small dosage of x₃. However, as x₁ dosage increases, the slurry PV reduces until x₁ reaches 23.5 g above which the PV tends to increase. A similar observation was noticed for the effects of the interaction between x₁ and x₂ on the FL (Figure 5b). The accelerator x₂ did not only impact the TT but also showed significant effects on the FL. The higher the dosage of x₂, the more the volume of the FL. It is also clear from Figure 5b that x₁ reduces the volume of FL when increased between 16-23.5 g above which the FL started to increase. The interaction of x₁ and x₂ as affecting cement Y_p revealed that the effect of x₁ on Y_p is relatively low when compared with the x₂. A high value of Y_p was recorded at minimum values of x₁ and x₂.



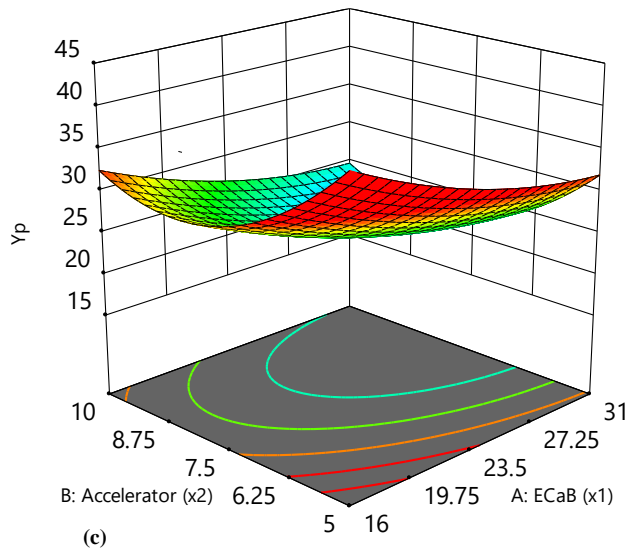


Figure 5: 3D graph showing the synergy between ECaB and other additives as they affect (a) PV, (b) FL and (c) Yp of cement slurry.

IV. MULTI-OBJECTIVE FUNCTION OPTIMIZATION STUDIES

To search for a combination of factor levels that satisfy the criteria placed on each of the responses, the optimization module in the Design Expert Version 11 was used. The fitted models for various responses obtained through the analysis of variance represent the objective function in the optimization. The constraints to the operation are the factors that are automatically included “in range”. Numerical optimization used the models to search the factor space for the best trade-offs to achieve multiple goals. In this case, the developed correlations were solved numerically by minimizing FL and maximizing the TT, CS, PV, and Yp subjected to x1(16-31 g), x2(0.5-1.4 g), and x3(5-10 g).

The objective function (Eqn. (5)) was automatically transformed to desirability (D). The overall desirability obtained after 1000 iterations is the multiplicative mean of all individual desirability (Eqn. (6)). The value of the desirability ranged between 0 and 1 where zero or low value of the desirability indicates a solution outside of the limits while a value of 1 indicates a solution at the goal. The input variables (x₁, x₂, and x₃) were adjusted numerically within range goals that keep the solution within the experimental boundaries. The numerical optimization finds a point that maximizes the desirability function given as:

$$D = \left(\prod_{i=1}^n d_i \right)^{\frac{1}{n}} \tag{6}$$

where *n* is the number of random sample and *d_i* is the desirability for different realizations.

At the optimum conditions x₁ (23.5 g), x₂ (7.5 g), and x₃ (0.95 g), the corresponding optimum TT, CS, PV, Yp, and FL are shown in Figure 6. These values were validated experimentally by experimenting with three replicates which yielded TT (228±16.4 min), CS₂₄ (614±0.57 psi), PV (17.5±1.35 cp), Yp (19.76±0.25 lb/100ft²) and FL (20 ml/30 min/100 psi). These values were found to agree with an

acceptable range as stipulated in the API RP 10B, (2012) and compare favourably to literature.

For example, Taylor and Iremonger, (2018), investigated the effect of glass microspheres on CS, TT, and FL properties of 11.27 ppg lightweight cement. A CS of 638 psi was reported after 48 h of curing at 72 °F and a strength of 1030 psi was obtained after curing for 7 days. A fluid loss of 25 ml after 30 min with no free water, and thickening time between 3–7 h were obtained. This result agrees perfectly with the present study. The TT of approximately 4 h and average FL of 20 ml/30 min/100 psi obtained in this study show that the slurry designed with 23.5 g ECaB blended cement enhanced the performance of the slurry. In our earlier study Arinkoola *et al.*, (2021), we reported that the TT for metakaolin and nanoclay fortified cement range from 334 – 492 minutes at 70 Bc. Although a much lower TT is recorded in the present study, the 4 h TT recorded falls within the acceptable range for cementing activities at shallow depth (Adjei and Elkatatny, 2021). If the TT is too short, the cement fails to reach its required placement, while too long a TT leads to costly delays or an increase of non-productive time Billingham *et al.* (2005). A similar investigation by Rageh *et al.* (2017) focused on the partial substitution of Portland cement with 2-12% imported bentonite. The authors recorded TT that ranged between 51-430 min and CS ranges between 420-2530 psi.

Abdullah *et al.* (2013) also reported a CS of 752 and 1405 psi after curing for 24 and 48h, respectively for a neat cement system. Although the average CS of 614 psi obtained in this present study is lower yet, CS higher than the formation pressure could fracture the formation. According to Adjei and Elkatatny, (2021), a minimum CS of 50 psi is sufficient to support the casing which agreed very well to the result from this study. The observations from this study also align well with Malyshev *et al.*, (2013). According to Malyshev *et al.*, approximately 250–1000 psi CS is sufficient to meet the requirement of many cementing operations. Not only that, for drilling out of the casing shoe, CS between 100–250 psi is sufficient while between 500–1000 psi is adequate to satisfy the demands of most cement operations.

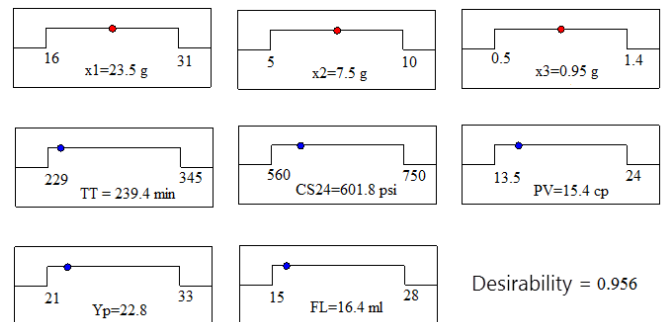


Figure 6: Optimum variables and the corresponding rheological and mechanical properties.

V. CONCLUSION

This study experimentally assessed the rheological and mechanical properties of Nigerian Ewu-Obi Calcium Bentonite (ECaB) as partial cement replacement for shallow depth cementing operations. It was established in this investigation that the selected clay from Ewu-Ebi deposit can be used as a replacement extender for class G cement in the production of reactive pozzolanic cement for concrete. The following conclusions can be drawn from the outcome of the investigation:

- i) The XRD analysis revealed that montmorillonite, kaolinite, Illite, and quartz are dominant minerals in the ECaB. The XRF analysis confirmed ECaB to be pozzolanic and therefore, a good candidate for strength development in concrete.
- ii) The optimum concentration of ECaB, accelerator and antifoam are 23.5 wt%, 7.5 wt%, and 0.95 wt%, respectively (by weight of cement).
- iii) The rheological properties i.e. the PV (17.5 ± 1.35 cp), Y_p (19.76 ± 0.25 lb/100ft²), and FL (20 ml/30 min/100 psi) obtained at optimum condition indicated that the cement slurry would remain pumpable with minimum fluid loss

The CS, and TT of slurry formulated at the optimum condition exhibit similar characteristics as those formulated with metakaolin, glass microspheres, and imported bentonite. The slurry is recommended for basic cementing operations for shallow and weak formations.

ACKNOWLEDGMENTS

The authors express gratitude to the management of SOWSCO Well Services (Nigeria) Limited, Rivers State, for the permission to use their chemical additives and equipment.

DECLARATION OF COMPETING INTEREST

The authors have no conflict of interest.

REFERENCES

- Abdullah, M. N.; D. Bedford; S. R. Wong and H. S. Yap. (2013).** Prehydrating High-strength Microspheres in Lightweight Cement Slurry Creates Value for Offshore Malaysian Operator. SPE Asia Pacific Oil and Gas Conference and Exhibition. doi:10.2118/165796-ms.
- Adjei, S. and Elkatatny, S. (2021).** Overview of the lightweight oil-well cement mechanical properties for shallow wells. Journal of Petroleum Science and Engineering, 198, 108201. doi:10.1016/j.petrol.2020.108201
- Adjei, S.; Elkatatny, S.; Sarmah, P.; and Abdelfattah, A. M. (2021).** Evaluation of calcined Saudi calcium bentonite as cement replacement in low-density oil-well cement system. Journal of Petroleum Science and Engineering, 205, 108901.
- Alkinani, H. H.; Al-Hameedi, A. T. T.; Flori, R. E.; Dunn-Norman, S.; Hilgedick, S. A.; Amer, A. S.; and Alsaba, M. T. (2018).** Drilling Strategies to Control Lost Circulation in Basra Oil Fields, Iraq, the 2018 AADE Fluids Technical Conference and Exhibition held at the Hilton Houston North Hotel, Houston, Texas, April 10-11.
- American Petroleum Institute. (2012).** Recommended practice for testing well cements 10B; 22-50. Washington, DC.
- Any, A. (2018).** Lightweight and Ultra-Lightweight Cements for Well Cementing - A Review. SPE Western Regional Meeting. doi:10.2118/190079-ms.
- API SPEC 10A, (2019).** Specification for Cements and Materials for Well Cementing. American Petroleum Institute.
- Arinkoola, A.O.; S.O. Alagbe, K.K Salam and B.M Ajagbe. (2022).** Performance of Oil Well Cement Slurry using Locally Sourced Extender. The Journal of Engineering Research (TJER), 19(1):73-84.
- Arinkoola, A. O.; Salam, K. K.; Alagbe, S. O.; Afolayan, A. S.; Salawudeen, T. O.; Jimoh, M. O. and Adeosun, T. A. (2021).** Influence of Metakaolin and nano-clay on compressive strength and thickening time of class G oil well cement. Songklanakarin Journal of Science & Technology, 43(1).
- ASTM C618-12a, (2010).** Standard Specification for Coal Fly Ash and Raw or Calcined Natural Pozzolan for Use. <https://doi.org/10.1520/C0618>.
- Billingham, J.; D. T. I. Francis; A. C. King and A. M. Harrison. (2005).** A Multiphase Model for the Early Stages of the Hydration of Retarded Oilwell Cement. Journal of Engineering Mathematics, 53(2), 99–112. doi:10.1007/s10665-005-9003-4.
- Bouaissi, A.; L. Y. Li; M. M. A. B. Abdullah; R. Ahmad; R. Abdul Razak and Z. Yahya. (2020).** Fly Ash as a Cementitious Material for Concrete. In Sustainable Building Materials; IntecOpen: 2020, DOI: 10.5772/intechopen.90466 .
- Cook, J., F. Growcock; Q. Guo; M. Hodder; E. Van Oort. (2011).** Stabilizing the wellbore to prevent lost circulation. Oilfield Rev. 23, 26–35.
- Elmarsafawi, Y. A.; R. Warman; A. Assad; M. M. Razouqi and F. Caillat. (2007).** Cementing a Producing Formation with Low-Fracture-Pressure Gradient in Wafra Field, Kuwait. Asia Pacific Oil and Gas Conference and Exhibition. doi:10.2118/107047-ms
- Fidan, E.; T. Babadagli and E. Kuru. (2004).** Use of Cement as Lost-Circulation Material: Best Practices. Canadian International Petroleum Conference. doi:10.2118/2004-090.
- Imbabi, M. S.; C. Carrigan and S. McKenna. (2012).** Trends and developments in green cement and concrete technology. International Journal of Sustainable Built Environment, 1(2), 194–216. doi:10.1016/j.ijbsbe.2013.05.001
- James, O. O.; M. M. Adediran; F. A. Adekola; E. O. Odebunmi and J. I. D. Adekeye. (2008).** Beneficiation and Characterisation of a Bentonite From North-Eastern Nigeria. Journal of the North Carolina Academy of Science, 124(4), 154–158.
- Lavrov, A. (2017).** Lost Circulation in Primary Well Cementing. Energy Procedia, 114, 5182–5192. doi:10.1016/j.egypro.2017.03.1672
- Magzoub, M.I.; S. Salehi, I.A.; Hussein and M.S. Nasser. (2020).** Loss circulation in drilling and well construction: the significance of applications of crosslinked polymers in wellbore strengthening: a review. J. Petrol. Sci. Eng. <https://doi.org/10.1016/j.petrol.2019.106653> .
- Malyshev, A.; T. Doronina, M. Popov, A. Ryabchikov, V. Shulga. (2013).** Optimized particles size

distribution lightweight cement at low temperatures: case study from eastern siberia, Russia. In: SPE Arctic and Extreme Environments Technical Conference and Exhibition, 15-17 October. Society of Petroleum Engineers, Moscow, Russia, pp. 627–652. <https://doi.org/10.2118/166849-ms>.

Morsy, M. S.; Y. A. Al-Salloum; H. Abbas and S. H. Alsayed. (2012). Behavior of blended cement mortars containing nano-metakaolin at elevated temperatures. *Construction and Building Materials*, 35, 900–905. doi:10.1016/j.conbuildmat.2012.04.099.

Shahriar, A. and Nehdi, M.L. (2012). Optimization of rheological properties of oil well cement slurries using experimental design. *Material Structure.*, 45(9): 1403-1423.

Rageh, S. M.; M. Z. Nezami; K. Dhanalakshmi and S. L. A. Basha. (2017). Compressive Strength and Thickening Time of Cement in Oil Well, *International Journal of Engineering Science Invention (IJESI)*, 6(12):1-4.

Taylor, J. and Iremonger, S. (2018). Design and Application of a New High Performance Lightweight Thermal Cement. SPE Thermal Well Integrity and Design Symposium. doi:10.2118/193350-ms.

Valcuende, M.; F. Benito, C. Parra and Miñano, I. (2015). Shrinkage of self-compacting concrete made with blast furnace slag as fine aggregate. *Construction and Building*

Materials, 76, 1–9. doi:10.1016/j.conbuildmat.2014.11.02910.1016/j.conbuildmat.2014.11.029

Wu, X.; F. Wan; Z. Chen; L. Han and Z. Li (2020). Drilling and completion technologies for deep carbonate rocks in the Sichuan Basin: Practices and prospects. *Natural Gas Industry B*. doi:10.1016/j.ngib.2020.09.012

Wang, C.; X. Chen; L. Wang; H. Ma; R. Wang. 2017. A novel self-generating nitrogen foamed cement: the preparation, evaluation and field application. *J. Nat. Gas Sci. Eng.* 44, 131–139. <https://doi.org/10.1016/j.jngse.2017.04.006>.

Xinniu, X. U.; S. U. N. Weiguo and R. U. A. N. Biao. (2019). Safe and fast drilling in ultradeep well at Dabasong uplift, Junggar Basin. *Drilling & Production Technology*, 42(6), 28-31.

Yuhuan B.; D. Jiapei; G. Shenglai; L. Huajie and Chenxing H. (2016). Properties of oil well cement with high dosage of metakaolin. *Construction and Building Materials*, 112: 39– 48. DOI: 10.1016/j.conbuildmat.2016.02.173

Yuhuan. B.; D. Jiapei; G. Shenglai; Huajie Liu and H. Chenxing. (2016). Properties of oil well cement with high dosage of MK. *Journal of Petroleum Science and Engineering*. Elsevier, 112:39-48.